Pérez, JJ.; González Suárez, A.; Nadal, E.; Berjano, E. (2020). Thermal impact of replacing constant voltage by low-frequency sine wave voltage in RF ablation computer modeling. Computer Methods and Programs in Biomedicine. 195:1-7. https://doi.org/10.1016/j.cmpb.2020.105673

Thermal impact of replacing constant voltage by low-frequency sine wave voltage in RF ablation computer modeling

Juan J. Pérez[1], Ana González-Suárez[2,3], Enrique Nadal[4], Enrique Berjano[1]

[1]BioMIT, Department of Electronic Engineering, Universitat Politècnica de València, Valencia, Spain, [2]Electrical and Electronic Engineering, National University of Ireland Galway, Ireland, [3]Translational Medical Device Lab, National University of Ireland Galway, Ireland, [4]Centro de Investigación en Ingeniería Mecánica, Universitat Politècnica de València, Valencia, Spain

Corresponding author: Enrique Berjano, Department of Electronic Engineering (Building 7F), Universitat Politècnica de València, Camino de Vera, 46022 Valencia, Spain.

Email: eberjano@eln.upv.es

Running head: Constant vs. low-frequency voltage in RFA modeling

Abstract

Background and objectives: A constant voltage (DC voltage) is usually used in radiofrequency ablation (RFA) computer models to mimic the radiofrequency voltage. However, in some cases a low frequency sine wave voltage (AC voltage) may be used instead. Our objective was to assess the thermal impact of replacing DC voltage by low-frequency AC voltage in RFA computer modeling.

Methods: A 2D model was used consisting of an ablation electrode placed perpendicular to the tissue fragment. The Finite Element method was used to solve a coupled electric-thermal problem. Quasi-static electrical approximation was implemented in two ways (both with equivalent electrical power): 1) by a constant voltage of 25 V in the ablation electrode (DC voltage), and 2) applying a sine waveform with peak amplitude of $25 \cdot \sqrt{2}$ V (AC voltage). The frequency of the sine signal (f_{AC}) varied from 0.5 Hz to 50 Hz.

Results: Sine wave thermal oscillations (at twice the f_{AC} frequency) were observed in the case of AC voltage, in addition to the temperature obtained by DC voltage. The amplitude of the oscillations: 1) increased with temperature, remaining more or less constant after 30 s; 2) was of up to ±3 ºC for very low f_{AC} values (0.5 Hz); and 3) was reduced at higher f_{AC} values and with distance from the electrode (almost negligible for distances > 5 mm). The evolution of maximum lesion depth and width were almost identical with both DC and AC.

Conclusions: Although reducing f_{AC} reduces the computation time, thermal oscillations appear at points near the electrode, which suggests that a minimum value of f_{AC} should be used. Replacing DC voltage by low-frequency AC voltage does not appear to have an impact on the lesion depth.

Key words: Computer modeling; quasi-static approximation; radiofrequency ablation.

1. Introduction

Radiofrequency (RF) ablation (RFA) is a minimally invasive procedure for a range of diseases, during which electrical current flows between an active electrode on the target site and a dispersive electrode on the patient's back. Due to its small size, current density is especially high around the active electrode and creates a thermal lesion exclusively in the target zone. Computer modeling has been shown to be a valuable tool for the study of the electrical and thermal performance of RFA. To solve the electrical problem associated with RFA models, quasi-static approximation is always used. From a mathematical point of view, this means that the RF voltage applied to each electrode, which is really a high-frequency (~500 kHz) sine waveform, is usually modeled as a constant voltage (DC voltage) with a value equivalent to the root-mean-square (RMS) value of the RF voltage (see Figure 1). This is because the RMS value of an alternating current (as is the case of RF) is the DC value when flowing through an electrical resistor produces the same amount of heat produced by the alternating current when flowing through the same resistor. This equivalence is valid, since in RFA biological tissue can be considered almost as a pure resistor because the displacement current is negligible against conduction current (in other words, $\sigma >> \omega \cdot \varepsilon$, σ being tissue electrical conductivity, ω the angular frequency associated with the RF signal, and ε tissue permittivity) [1].

Although DC voltage is common in most RFA models, in some cases a low frequency AC voltage (at frequency f_{AC}) may be used instead, especially in the context of phase-shifted RFA models [2,3]. Phase-shifted mode is based on applying RF power

simultaneously through several active electrodes so that the sine waveform voltages applied by each electrode have the same frequency and amplitude but a different initial phase angle, i.e. they are displaced in a time domain, which means that the electrode voltage is set as an alternating current voltage (AC voltage) with specific values for amplitude, frequency, and phase angle [2,3] (see Fig. 1). Although this method has been called 'transient approximation' by some authors [3], we think that it really comes within the scope of the quasi-static approximation, the reason being that quasi-static approximation goes a little further, since it not only refers to keeping the electrical parameters static (voltage and current) but also to varying them slowly over time. In our context 'slowly' means that the solution of the electrical problem can be obtained by assuming that the voltage applied in the electrodes is independent of time (even though it really changes), i.e. by solving a static problem at every instant that the voltage applied to the electrode changes. This is true in the case of RFA, in which the wavelength is huge compared to the distance between the electrodes [1]. In terms of mathematical equations this means that it is not necessary to solve the electromagnetic wave equation and that the electrical problem is solved using the equation $\nabla\cdot(\sigma\ \nabla\Phi)=0$ where Φ is the voltage at any point. The magnitude of the vector electric field $\boldsymbol{E}$ (V/m) is then obtained from $\boldsymbol{E} = -\nabla\Phi$. Strictly speaking, quasi-static approximation is always employed for RFA models, for either a constant voltage value to mimic the RMS value of the true sine waveform corresponding with the RF signal or if we change the electrode voltages according to the same RF sine waveform. To sum up, quasi-static approximation can be used to model RFA using both DC and AC voltages.

The problem of applying AC voltage as a load on the ablation electrode is that the time-step has to be drastically reduced, since the value of the voltage takes several values within

each cycle or period, which unquestionably considerably increases the required computation time. In order to keep this time reasonably low, previous studies used a sine wave with 0.5 Hz frequency instead of the true RF signal (500 kHz) [2,3]. Although the authors claimed that this method is valid to model RFA, the thermal impact of using AC instead of DC voltage has not yet been assessed. Our objective was thus to compare the temperature distributions obtained by using a low-frequency AC voltage plus a DC voltage in an RFA computer model.

2. Methods

2.1. Model geometry

Although AC-voltage has been especially proposed for phase-shifted RFA models, we considered here a generic case of RF cardiac ablation based on a previous model [4]. Figure 2(a) shows the geometry and dimensions of the considered two-dimensional computational model, consisting of an active electrode (4 mm, 7 Fr) perpendicular to the tissue surface and inserted to a depth of ~0.4 mm in the tissue. The dispersive electrode was modeled as a boundary condition on the bottom surface of the tissue. Cardiac tissue and blood chamber dimensions (X, Y and C) were estimated by means of a convergence test to avoid boundary effects. In this test, the value of the maximum temperature in the tissue (T_{max}) after 120 s of RF heating was used as a control parameter. We first considered a tentative spatial (i.e. minimum meshing size) and temporal resolution. To determine the appropriate parameters we increased their values by equal amounts. When the difference in the T_{max} between consecutive simulations was less than 0.5% the former values were considered to be adequate. We then determined the appropriate spatial resolution by means of a similar

convergence test using the same control parameters as in the previous test. Discretization was spatially heterogeneous: the finest zone was always the electrode-tissue interface, in which the largest voltage gradient was produced and hence the maximum value of current density. The grid size was gradually increased in the tissue with distance from the electrode-tissue interface.

2.2. Governing equations

The computer model was based on a coupled electric-thermal problem which was solved numerically using the Finite Element Method (FEM) with ANSYS software (ANSYS, Canonsburg, PA, USA). The governing equation for the thermal problem was the Bioheat Equation [5]:

$$\rho c \frac{\partial T}{\partial t} = \nabla \cdot (k \nabla T) + q - Q_p + Q_m \quad (1)$$

where ρ is density (kg/m^3), c specific heat (J/kg·K), T temperature (ºC), t time (s), k thermal conductivity (W/m·K), q the heat source caused by RF power (W/m^3), Q_p the heat loss caused by blood perfusion (W/m^3) and Q_m the metabolic heat generation (W/m^3). Both Q_m and Q_p were ignored as these terms are negligible compared to the others [4,5]. A quasi-static approximation was employed for the electrical problem. The magnitude of the vector electric field $\boldsymbol{E}$ was obtained from $\boldsymbol{E} = -\nabla V$ (V being voltage) while voltage was obtained from $\nabla \cdot (\sigma(T) \nabla V) = 0$ (σ being electrical conductivity). The distributed heat source q was then obtained as $q = \sigma |\boldsymbol{E}|^2$. The thermal expansion effect was not taken into account since it is generally ignored in RFA modeling and is possibly more influential in simulating microwave ablation, which reaches higher tissue temperatures [6].

We chose the Bioheat Equation to model heat transfer. Although this model is widely accepted as reliable for bioheat transfer, other models have been proposed through the years to overcome some limitations, such as the direction of the blood flow [7–9]. Some of these alternatives, e.g. the one based on porous media theory, have even been applied to RF cardiac ablation [10]. It should be noted that our conclusions could vary if other bioheat models were to be considered.

2.3. Model properties and boundary conditions

The thermal and electrical properties of the model elements are shown in Table 1 [3,4]. The initial temperature in the entire model was T_0 = 37 ºC. The electrical (σ) and thermal (k) conductivity of cardiac tissue were considered as a temperature-dependent function as follows: σ rose exponentially +1.5%/ºC, i.e. $\sigma(T) = \sigma_0 \cdot e^{0.015 \cdot (T - T_0)}$, σ_0 being the electrical conductivity at 37 ºC. And k rose linearly +1.2%/ºC i.e. $k(T) = k_0 \cdot (1 + 0.012 \cdot (T - T_0))$, k_0 being the thermal conductivity at 37 ºC [4]. No change associated with vaporization was modeled since tissue temperatures were always below 90 ºC.

Figure 2(b) shows the electrical and thermal boundary conditions. A null thermal flux was used for the thermal boundary conditions on the symmetry axis and a constant temperature of 37 ºC was fixed on the outer surfaces of the model at a distance from the ablating electrode (this was also the initial temperature value). The effect of blood circulating inside the cardiac chamber was modeled by thermal convection coefficients at the electrode–blood (h_E) and tissue–blood (h_T) interfaces, considering electrical conductivity of blood to be independent of temperature and high blood flow conditions (h_E = 3346 W/m^2·K and h_T = 610 W/m^2·K) [4]).

A Dirichlet voltage boundary condition was applied at the active electrode for the electrical boundary conditions. Although RF cardiac ablation is currently conducted using constant power or constant temperature, we used a constant-voltage mode since it was simpler and more suitable for our purpose. An RMS value of 25 V was chosen to create significant thermal lesions after 60 s while avoiding overheating (temperature around 100 ºC). All the outer surfaces of the model except the bottom surface were fixed at zero electric flux (Neumann boundary condition). The voltage on the bottom surface was set to 0 V (dispersive electrode).

2.4. DC vs. AC voltage

Quasi-static approximation was implemented in two different ways: 1) fixing a constant voltage at the active electrode $\Phi_E = V_{DC} = 25$ V in the ablation electrode (DC case) (see Fig. 1), and 2) applying a sine waveform V_{AC} whose amplitude (peak value) was $25 \cdot \sqrt{2}$ V (AC case), i.e. a time-dependent voltage $\Phi_E(t) = 25 \cdot \sqrt{2} \cdot sin(2 \cdot \pi \cdot f_{AC} \cdot t)$. In this way both cases had the same RMS value and theoretically equal applied energy. In the AC case, we conducted computer simulations changing the frequency of this sine waveform signal from a low value of 0.5 Hz (already employed in a previous modeling study [2,3]) to a value 100 times bigger (50 Hz) and analyzed its impact on the temperature at different depths and lesion size. Note that since applied power is given by $P = \Phi_E^2/Z$ (Z being impedance), the instantaneous power in the AC case is $P(t) = \Phi_E^2(t)/Z(t) = [25 \cdot \sqrt{2} \cdot sin(2 \cdot \pi \cdot f_{AC} \cdot t)]^2/Z(t)$, which is the signal at frequency $2 \times f_{AC}$ (see Fig.1).

In terms of electrical boundary conditions, the sine wave was initially generated using 40 points/period, so that the time interval between points was $\Delta t = T/40$, T being the period

of each sinus. Note that Δt was not related to the time-step used internally by ANSYS to obtain the solution, which was obviously smaller than this value. Additionally, we were interested in studying the impact of a lower number of points/period, since this has a direct impact on computation time. For instance, we initially employed 40 points/period (as in Yan *et al.* [3]) while Tungjitkusolmun *et al.* [2] used 17 points/period). To assess this effect, we ran simulations of 120-s RF ablation with AC voltage (f_{AC} = 0.5 Hz) and changed the points/period from 10 to 40.

2.5. Output variables

Temperature evolution during ablation was monitored at different depths from the electrode surface (0.1 to 10 mm) together with lesion size (maximum width and depth) by the Arrhenius damage model [5], which associates temperature with exposure time using a first-order kinetics relationship:

$$\Omega(t) = \int_0^t A e^{-\frac{\Delta E}{R \cdot T}} ds \qquad (2)$$

where R is the universal gas constant (8.314 J/K mol), A (2.94×10^{39} s^{-1}) is a frequency factor and ΔE (2.596×10^{5} J/mol) is the activation energy for the irreversible damage reaction. The values of these parameters had been used in a previous RF cardiac ablation computer model [11] derived from experiments in which an assessment was made of the changes in tissue optical properties caused by heating [12]. These values are therefore not directly related to damage at the cellular level, i.e. Ω = 1 (used here to estimate the lesion boundary) and do not necessarily mean there is exactly a 63% probability of cell death.

However, this limitation can be ignored since Eq. (2) was only used to compare the lesion size obtained using DC and AC voltages and not for prediction purposes.

3. Results

After conducting a convergence test we obtained the following optimum values for the main geometrical parameters of the model: X=Y=40 mm, and C=40 mm. These values have previously been shown to acceptably represent the real situation in RF cardiac ablation [13]. The time intervals used to synthesize the sine signal varied with f_{AC} (see Methods section) from 100 ms for 0.5 Hz to 1 ms for 50 Hz. This was not the interval of the time-step used internally by ANSYS to obtain the transient solution, which was variable and always much smaller (e.g. ~0.03 ms for f_{AC} = 50 Hz). The model had nearly 17,000 triangular elements (36,800 nodes). The optimal mesh size was 0.2 mm around the active electrode and ~7 mm around the dispersive electrode.

Figure 3 shows temperature evolution in the tissue at 0.2 mm from the electrode using an AC voltage with f_{AC} = 0.5 Hz and DC voltage. The most important finding is the existence of sine waveform thermal oscillations in the AC case with a frequency value twice that of the f_{AC}. The oscillations were also found at other points around the electrode and were especially noted at 0.2 mm. The amplitude of this oscillation (assessed as peak to peak value) rose slightly with heating, e.g. from 6.7 ºC at 10 s to 7.6 ºC at 30 s, after which it remained more or less constant. The average value in the AC case was identical to the temperature obtained with DC (blue line in Fig. 3). Figure 3 also shows the temperature evolution in the electrode, at 1 mm from the tissue, which is the typical distance where a

temperature sensor is sometimes located in the case of constant temperature ablation. It is noteworthy the fact that thermal oscillations also appear at this point in the AC case.

Figure 4 shows temperature evolution at 0.2 mm from the electrode for different f_{AC} values. The simulations were only run for 30 s since the thermal oscillations were seen to be more or less stable after this point. The peak-to-peak value of the thermal oscillations fell when f_{AC} rose. The frequency of the oscillations was twice the value of the corresponding f_{AC} and all the plots had the same mean value. Computation time increased drastically for a 30-s ablation when f_{AC} rose: from 24 minutes for 0.5 Hz up to 7.5 days for 50 Hz (only 18 minutes for DC).

Figure 5 shows the peak-to-peak values of the thermal oscillations after 30 s of RFA for different f_{AC} values and distance from the electrode. Thermal oscillation can be seen to fall with distance while f_{AC} rises. Exceptionally, maximum amplitude occurs at 2 mm at low f_{AC} values instead of closer to the electrode (1 mm). There are no oscillations at distances greater than 5 mm, regardless of f_{AC}. Above 10 Hz the thermal oscillations are below 1 ºC for f_{AC}.

Figure 6 shows temperature evolution at different electrode distances during the reduction of the points/period from 40 to 10. Only the last 5 s of the ablation is shown. The use of 10 points can be clearly seen to delay the thermal oscillations and reduce their amplitudes (see plots at 0.1–0.5 mm), and finally reduces the mean temperature at deeper points (see plots at 1–5 mm). The results shown in Fig. 6 also confirm that the number of points/period chosen to synthesize the sine waveform is not related to the thermal oscillations itself.

Figure 7 shows the thermal lesion size evolution from the Arrhenius damage model for

f_{AC} = 0.5 Hz, which can be considered to be the worst case in terms of thermal oscillation amplitude. The maximum lesion width and depth computed from DC and AC were seen to be almost identical.

4. Discussion

4.1. Thermal impact of replacing constant voltage by low-frequency sine wave voltage

This study explored the effect of using a low frequency sine waveform voltage to model phase-shifted multielectrode RF cardiac ablation, the reason being that constant voltage cannot be used to model RF voltage, as in conventional RF ablation or in duty-cycled multielectrode ablation. To date, low frequency f_{AC} (instead of RF) has been used only because it reduces computation time [2,3]. Our results showed that when f_{AC} is low (< 10 Hz) the temperature evolution near the electrode (1–2 mm) has frequency oscillations twice those of f_{AC} (see Fig. 3–5). This double frequency comes from the quadratic value of the sine waveform voltage, which is proportional to the applied power and hence to the heating effect.

The amplitude of these oscillations is by no means negligible, since it can cause temperature variations of up to ± 3 ºC when f_{AC} is extremely low (0.5 Hz). In practical terms, although the lower f_{AC} reduces computation time significantly, it has the drawback of adding oscillations to the temperature evolution at points near the electrode, indicating that f_{AC} should have a minimum value of 10 Hz in order to avoid excessive oscillations (higher than 1 ºC peak-to-peak).

The plots shown in Fig. 5 (with the f_{AC} value on the abscissa axis) summarize all the results in terms of oscillation amplitude and could be interpreted as a Bode diagram on the

thermal response at different electrode distances. The behavior of the plots in Fig. 5 suggests a sort of spatial low-pass filter, i.e. the oscillation amplitude decreases when f_{AC} increases and also with electrode distance, which makes sense if we think of the thermal behavior of biological tissue as a combination of (thermal) resistance in parallel with a capacitor (heat capacity), i.e. as the oscillating part of the heat flows through the tissue, its amplitude is reduced (distance dampens the effect of the oscillations).

The results obtained also show no difference in the evolution of lesion size between DC and AC, regardless of f_{AC}. This is in line with the fact that the mean temperature value at the points affected by thermal oscillations was identical to the temperature computed from the DC voltage. This softens the requirement that the f_{AC} be sufficiently high to avoid thermal oscillations if the only interest is lesion size. However, if the interest is in maximum tissue temperature (which could be associated with steam pops [14]), the f_{AC} value should be sufficiently high, basically above 10 Hz, to avoid oscillations higher than 1 ºC or even above 20 Hz to avoid oscillations higher than 0.5 ºC. The frequency value employed in previous studies, 0.5 Hz [2,3], thus seems excessively low to study the temperature values reached in the tissue, as reported by Yan *et al* [3]. Moreover, the oscillations provoked by an excessively low f_{AC} value also affect the temperature measurement point (see Fig. 3) and could hence alter the controller performance when we are modeling a constant temperature ablation.

About the effect of the points/period employed to mathematically build the sine waveform signal in the case of AC voltage, our results show that when the points/period number is only 10, temperature at some points can drop by up to 5 ºC (Fig. 6). This loss is due to the reduction of applied power when the sine waveform is built with few segments.

The square of the RMS value of a sine signal changes when this wave is synthesized using *n* linear segments and this can be mathematically calculated. In the extreme case of *n*=3 (it is really a triangular wave, instead of a sine), the square of the RMS value is 50% lower than the case of the pure sine wave (infinite points), while the reduction is only 0.4%, 0.8%, 1.7% and 6.4% when we take 40, 30, 20 and 10 points/period, respectively. This reduction is directly related to the applied power (which is proportional to the square of the RMS value) and hence it should be taken into account when the sine signal is synthesized in steps. In order to avoid this 'loss of applied power' the results suggest that the sine waveform AC voltage should be built with at least 20 points/period.

4.2. Model validation and verification

It is important to point out that we do not propose any new model, but we used a model that had previously been validated in numerous studies (e.g. [15–17]), and which was based on a well-known physical-mathematical framework (Laplace Equation and Bioheat Equation). In other words, these equations, along with the material properties, accurately represent the real physical event of the RFA [18]. Also, our particular model was verified in terms of spatial (mesh size) and time (time-step) discretization, along with the outer dimensions. Convergence tests were conducted to verify that the values used in the computer model represented the RFA mathematical model of the RFA with sufficient accuracy [18]. The meshing size at the electrode-tissue interface was ~0.02 mm and at the point furthest from the active electrode was ~2 mm. The optimal time-step was ~0.07 s and the number of elements was around 14,400. Note that our objective was precisely to determine how a much lower frequency AC voltage than that used in a real physical situation (500 kHz)

cannot verify the model in terms of temperature at points near the active electrode, since the thermal oscillations have not been seen in previously validated DC voltage-based models.

4.3. Limitations of the study

In order to explore the thermal effect of using a low-frequency sine voltage for RFA we used a simple model based on a single active electrode. In a real physical scenario phase-shifted multi-electrode RFA requires more than one active electrode, since a phase angle has to be set between the voltages applied at each active electrode. The model chosen was based on a simple electrode because this allowed a clearer analysis of the relevant factors (f_{AC} value and distance from the electrode) and the results in terms of temperature and lesion size evolution. We considered that a model with different phase angles between the electrodes could mask the effect of the f_{AC}. Of course we recognize that our conclusions are qualitatively general and valid, i.e. in terms of the relationships between the f_{AC} value, thermal oscillation amplitude and lesion size, which means that the quantitative details will obviously depend on the particular model in question. Our findings should serve to alert researchers who replace DC voltage with low frequency AC voltage in RFA models.

As a protocol based on constant voltage was used, i.e. the voltage applied to the active electrode did not depend on tissue impedance, the applied power changed with tissue impedance from the initial 8.9 W (~70 Ω tissue impedance) to 9.3 W at 30 s (67 Ω tissue impedance). Although other protocols are clinically employed in RF cardiac ablation (such as constant power and constant temperature), we consider the chosen model valid for this objective and do not believe that the conclusions would vary if other protocols were used. Also, the applied energy was almost identical in both cases, since the thermal oscillations

have such a small amplitude that the changes in electrical conductivity were almost identical. For instance, the energy applied for 120 s was 1.110 kJ in the DC case and 1.115 kJ in the AC (mean power 9.26 W and 9.29 W, respectively). We can thus assume that the total energy was the same in all the cases considered.

Although the results suggest that the use of low frequency sine waveform voltage does not have drawbacks if the interest is in thermal lesions (not tissue temperature) this may not be the case if the simulation reaches vaporization temperatures, where the tissue characteristics change abruptly on reaching the threshold value (around 100 °C). In this case, lesion size could vary with the amplitude of the oscillations, i.e. the exact value of the f_{AC} used.

Instead of solving the fluid dynamics problem we used the heat transfer coefficient to model the thermal effect of the circulating blood. In spite of this limitation, we have previously shown that this approximation can predict lesion depth and tissue temperature reasonably well [19]. However, since it cannot predict lesion width so well (specially the surface width), the specific result shown in Fig. 7B could vary slightly if blood motion is included in the model.

This study only considered an electrode perpendicular to the tissue. Although electrodes can be placed at other angles during RF cardiac ablation, there is no physical reason to expect that our conclusions will change at other angles. We chose 90º since it allowed a 2D model and simulations with a high f_{AC} value required a reasonable computation time. We only focused on non-irrigated electrodes. Although irrigated-tip electrodes are commonly used for in RF cardiac ablation for atrial fibrillation, dry electrodes are widely used for many other RF ablation techniques. Our results show that thermal oscillations are greater in

the vicinity of the electrode (Fig. 5). Since the irrigated electrodes "push" the hottest point into the tissue, the oscillation amplitude is likely to be smaller for irrigated electrodes. In any case, it does not seem that the conclusions from dry and irrigated electrodes will be qualitatively different. It is also reasonable to assume that our conclusions could be equally valid for other RFA models (not only RF cardiac ablation), at least qualitatively, due to: 1) the existence of sine wave thermal oscillations specially noticeable when f_{AC} is low, 2) reducing the amplitude of these oscillations with distance from the electrode, and 3) not affecting lesion size.

5. Conclusions

When DC voltage is replaced by AC voltage in RFA computer modeling and the the AC voltage sine waveform frequency is too low (≤ 10 Hz), thermal oscillations of up to ±3 ºC appear in the temperature computed at points near the electrode (< 5 mm). Maximum lesion width and depth evolution is identical to that computed by a constant voltage, i.e. the oscillations do not have an impact on the thermal lesion size.

Acknowledgements

This work was supported by the Spanish *Ministerio de Ciencia, Innovación y Universidades* under "*Programa Estatal de I+D+i Orientada a los Retos de la Sociedad*", Grant Nº "RTI2018-094357-B-C21". The authors have no conflicts of interest or financial disclosures to make relevant to this submission.

References

1. Doss JD. Calculation of electric fields in conductive media. Med Phys 1982;9(4):566−73.
2. Tungjitkusolmun S, Haemmerich D, Cao H, Tsai JZ, Choy YB, Vorperian VR, Webster JG. Modeling

bipolar phase-shifted multielectrode catheter ablation. IEEE Trans Biomed Eng. 2002 Jan;49(1):10-7.
3. Yan S, Wu X, Wang W. A simulation study to compare the phase-shift angle radiofrequency ablation mode with bipolar and unipolar modes in creating linear lesions for atrial fibrillation ablation. Int J Hyperthermia. 2016 May;32(3):231-8.
4. Pérez JJ, González-Suárez A, Berjano E. Numerical analysis of thermal impact of intramyocardial capillary blood flow during radiofrequency cardiac ablation. Int J Hyperthermia. 2018 May;34(3):243-9.
5. Berjano EJ. Theoretical modeling for radiofrequency ablation: state-of-the-art and challenges for the future. Biomed Eng Online 2006;5:24.
6. Keangin P, Wessapan T, Rattanadecho P. Analysis of heat transfer in deformed liver cancer modeling treated using a microwave coaxial antenna. Applied Thermal Eng, 2011. 31(16):3243-54.
7. Nakayama A, Kuwahara F. A general bioheat transfer model based on the theory of porous media. International Journal of Heat and Mass Transfer, 2008. 51(11-12):3190-3199.
8. Bhowmik A, Singh R, Repaka R, Mishra SC. Conventional and newly developed bioheat transport models in vascularized tissues: A review. Journal of Thermal biology, 2013. 38(3):107-125.
9. Andreozzi A, Brunese L, Iasiello M, Tucci C, Vanoli GP. Modeling heat transfer in tumors: a review of thermal therapies. Ann Biomed Eng, 2019. 47(3):676-693.
10. Iasiello M, Andreozzi A, Bianco N, Vafai K. The porous media theory applied to radiofrequency catheter ablation. International Journal of Numerical Methods for Heat & Fluid Flow, Vol. 30 No. 5, pp. 2669-2681. https://doi.org/10.1108/HFF-11-2018-0707.
11. González-Suárez A, Herranz D, Berjano E, Rubio-Guivernau JL, Margallo-Balbás E. Relation between denaturation time measured by optical coherence reflectometry and thermal lesion depth during radiofrequency cardiac ablation: feasibility numerical study. Lasers Surg Med. 2018 Mar;50(3):222-29.
12. Jacques SL, Gaeeni MO. Thermally induced changes in optical properties of heart. Annual International Conference of the IEEE Engineering in Medicine and Biology – Proceedings. 1989. 11(Pt. 4): 1199–1200.
13. Irastorza RM, Gonzalez-Suarez A, Pérez JJ, Berjano E. Differences in applied electrical power between full thorax models and limited-domain models for RF cardiac ablation. Int J Hyperthermia. 2020;37(1):677-687. doi: 10.1080/02656736.2020.1777330.
14. Seiler J, Roberts-Thomson KC, Raymond JM, Vest J, Delacretaz E, Stevenson WG. Steam pops during irrigated radiofrequency ablation: feasibility of impedance monitoring for prevention. Heart Rhythm. 2008 Oct;5(10):1411-6.
15. González-Suárez A, Berjano E, Guerra JM, Gerardo-Giorda L. Computational modeling of open-irrigated electrodes for radiofrequency cardiac ablation including blood motion-saline flow interaction. PLoS One. 2016 Mar 3;11(3):e0150356.
16. Bourier F, Duchateau J, Vlachos K, Lam A, Martin CA, Takigawa M, Kitamura T, Frontera A, Cheniti G, Pambrun T, Klotz N, Denis A, Derval N, Cochet H, Sacher F, Hocini M, Haïssaguerre M, Jais P. High-power short-duration versus standard radiofrequency ablation: Insights on lesion metrics. J Cardiovasc Electrophysiol. 2018 Nov;29(11):1570-1575.
17. Labonté S. Numerical model for radio-frequency ablation of the endocardium and its experimental validation. IEEE Trans Biomed Eng. 1994 Feb;41(2):108-15.
18. Babuska I, Oden JT. Verification and validation in computational engineering and science: basic concepts. Comput. Methods Appl. Mech. Engrg. 2004; 193:4057–66.
19. González-Suárez A, Pérez JJ, Berjano E. Should fluid dynamics be included in computer models of RF cardiac ablation by irrigated-tip electrodes? Biomed Eng Online. 2018 Apr 20;17(1):43. https://doi.org/10.1186/s12938-018-0475-7.

Table 1 Physical characteristics of tissues and materials employed in the computational models (data from [3,4]).

Tissue	σ **(S/m)**	k **(W/m·K)**	ρ **(kg/m^3)**	c **(J/kg·K)**
Cardiac tissue	0.54	0.53	1060	3111
Cardiac chamber/Blood	0.99	0.54	1000	4180
Electrode/Pt-Ir	4.6×10^{6}	71	21500	132
Catheter/Polyurethane	10^{-5}	0.026	70	1045

σ: electric conductivity; k: thermal conductivity; ρ: density; c: specific heat (assessed at 37 ºC)

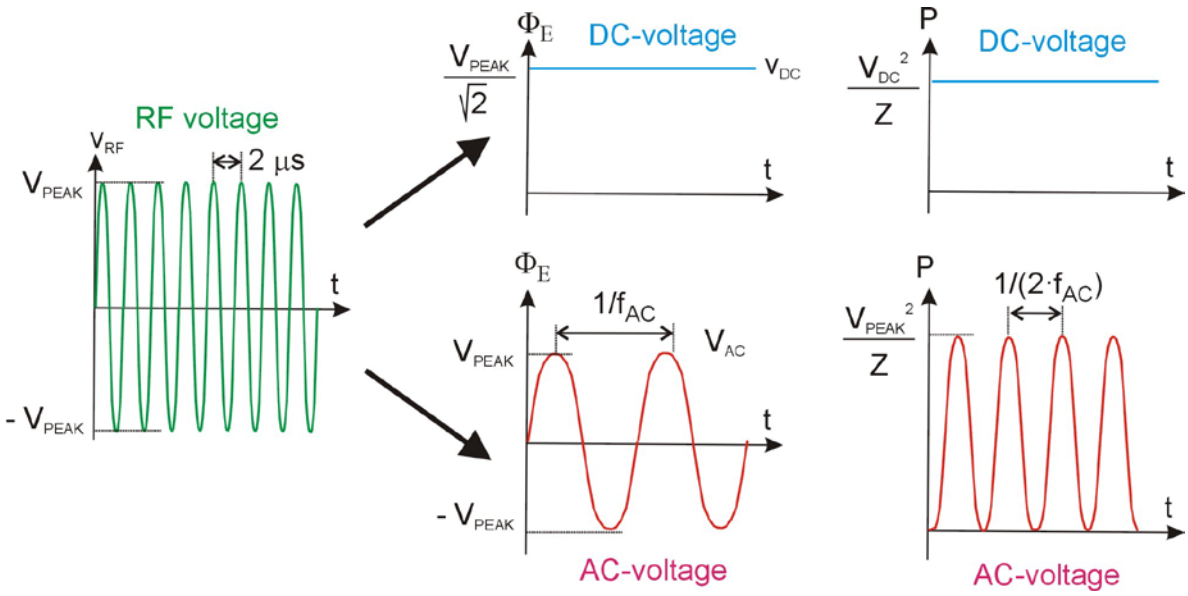

Figure 1 Computer modeling of RF ablation always simplifies the electrical problem by using the quasi-static approximation, which substitutes the RF voltage (V_{RF}) either for a constant voltage (V_{DC}) or for alternating voltage (V_{AC}), both applied as a load Φ_E on the active electrode. V_{AC} frequency (f_{AC}) is always much lower than RF frequency (500 kHz) to reduce computation time. The V_{DC} value has to be equal to the root-mean-square (RMS) value of the RF voltage. When the waveform is a pure sine wave (as in RFA), the RMS value is equal to peak amplitude (V_{PEAK}) divided by $\sqrt{2}$. The electrical power P applied is the product of the squared voltage divided by the impedance of the tissue Z. In the case of AC-voltage, the square of V_{AC} is a squared sine signal, which has twice the f_{AC} frequency.

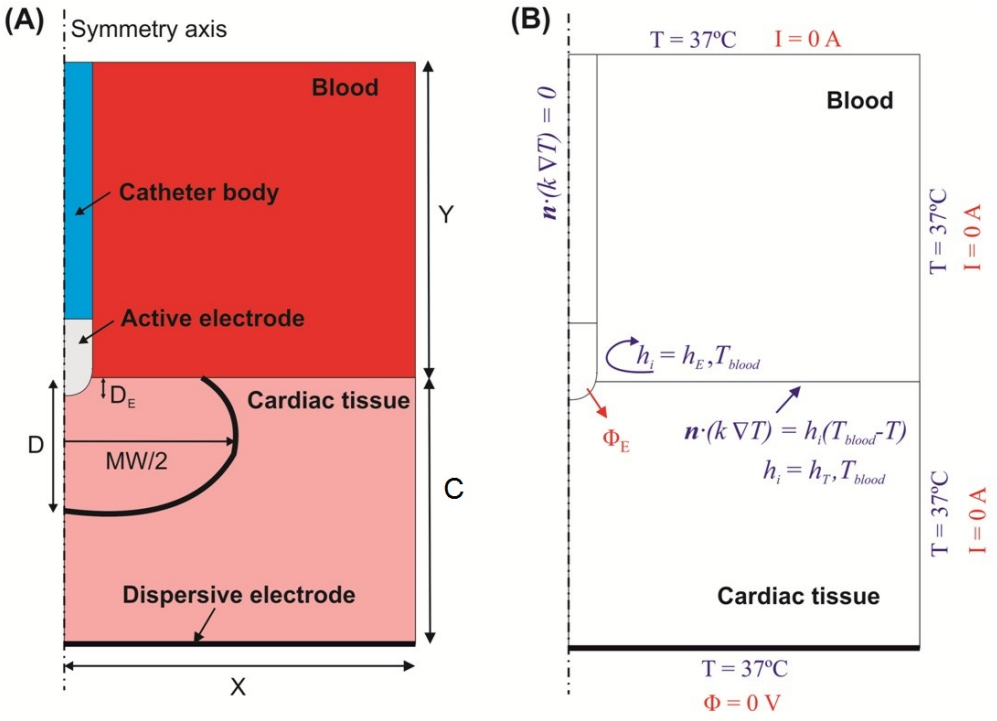

Figure 2 **(A)** Geometry of the two-dimensional computational model built (not to scale) including an ablation electrode (7Fr, 4 mm) inserted 0.4 mm into a fragment of tissue and completely surrounded by blood. Dimensions of cardiac tissue and blood (X, Y and C) were obtained from a convergence test. **(B)** Electrical (red) and thermal (blue) boundary conditions of the model. h_E and h_T are the thermal convection coefficients at the electrode–blood and tissue–blood interfaces, respectively. While the voltage Φ at the dispersive electrode (bottom) was always set to 0 V, its value on the active electrode depended on the approximation employed: 25 V with 'DC voltage' or a sine voltage with different f_{AC} frequency values with 'AC voltage'.

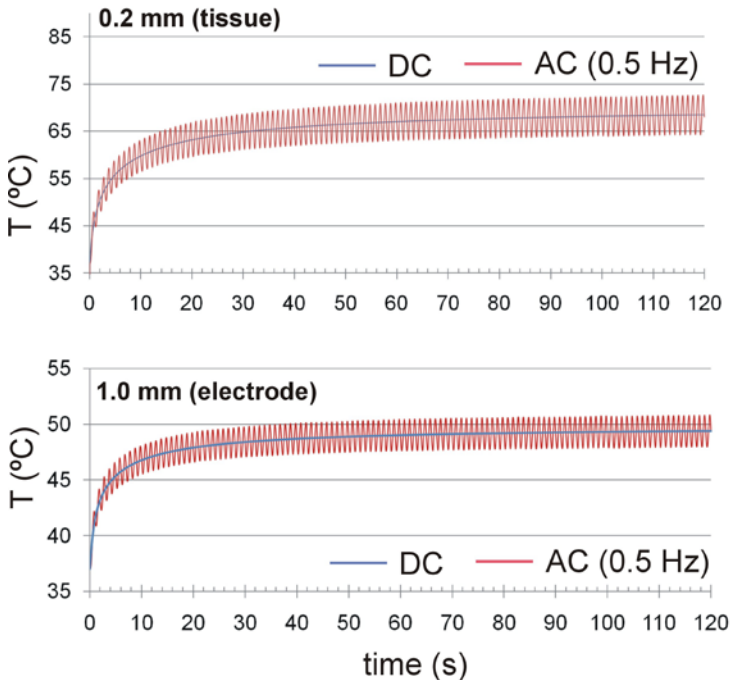

Figure 3 Temperature evolution in the tissue at 0.2 mm from the electrode (top) and in the electrode at 1 mm from the tissue (bottom) with AC voltage at f_{AC} = 0.5 Hz (red line) and a DC voltage (blue line). The average value with AC is identical to the temperature obtained with DC.

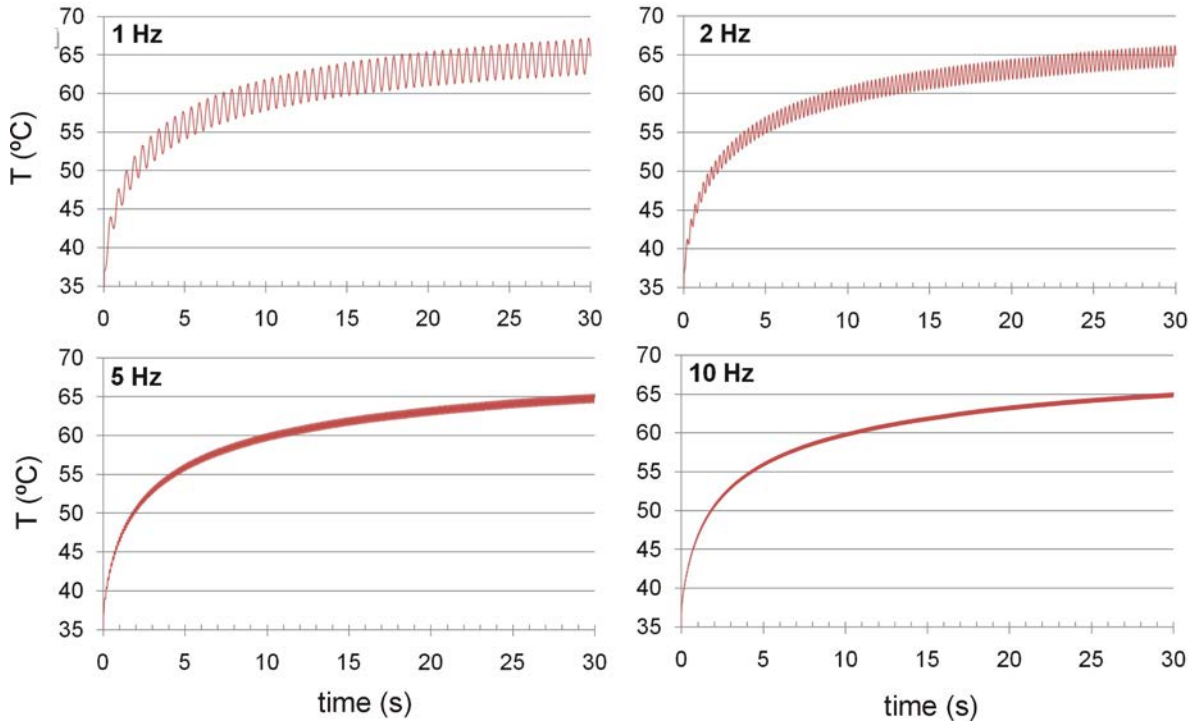

Figure 4 Temperature evolution at 0.2 mm from the electrode using AC voltages at different f_{AC} values (1 Hz to 10 Hz).

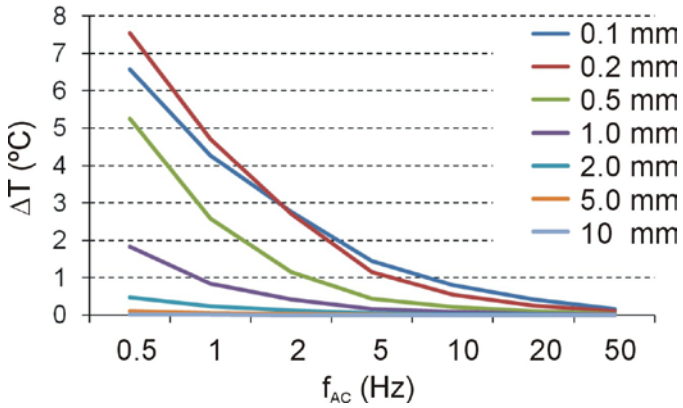

Figure 5 Peak-to-peak values of temperature oscillations at 30 s of RF ablation with AC for different frequencies (f_{AC}) and distance from the electrode.

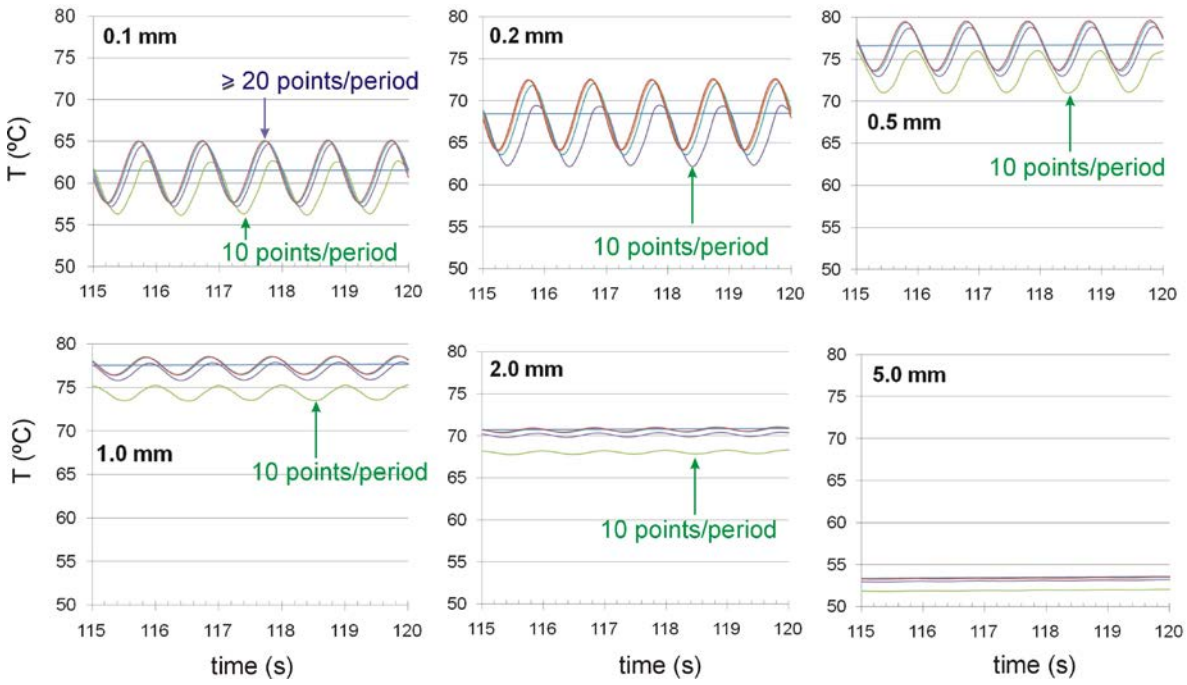

Figure 6 Temperature evolution (for the last 5 s of ablation) at different distances from the electrode (0.1–5.0 mm) with AC at f_{AC} = 0.5 Hz and different points/period. Only the case with 10 points/period (green line) shows delayed thermal oscillations and reduced amplitudes.

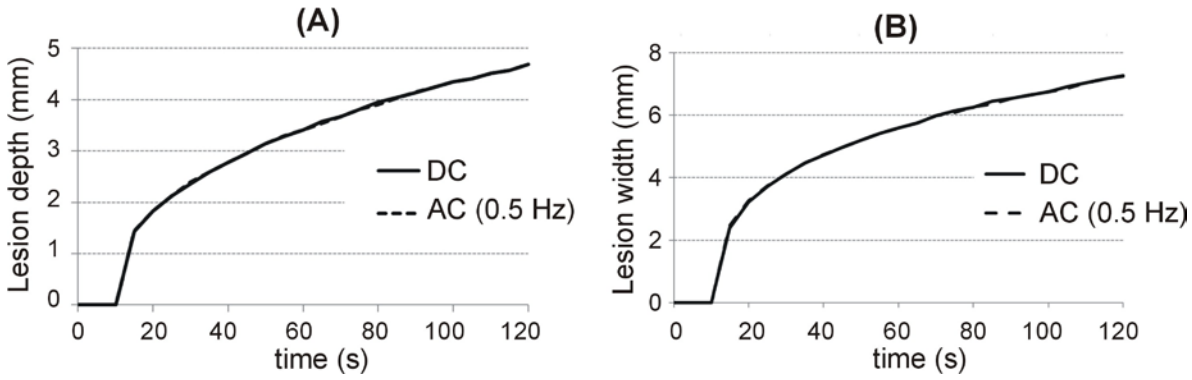

Figure 7 Evolution of lesion depth (A) and surface width (B) during 120-s RF ablation with DC (solid line) and AC (dashed line). A constant value of 25 V was used for DC, while a sine waveform voltage with a peak value of $25 \cdot \sqrt{2}$ V and f_{AC} = 0.5 Hz was used with AC. Both lines practically overlap.